US012385733B2

(12) **United States Patent**
McMorrow et al.

(10) **Patent No.: US 12,385,733 B2**
(45) **Date of Patent: Aug. 12, 2025**

(54) **SYNCHRONIZING AN OPTICAL COHERENCE TOMOGRAPHY SYSTEM**

(71) Applicant: **VerAvanti Inc.**, Redmond, WA (US)

(72) Inventors: **Gerald McMorrow**, Redmond, WA (US); **Jongtae Yuk**, Redmond, WA (US)

(73) Assignee: **SOHAM INC.**, Bellevue, WA (US)

(*) Notice: Subject to any disclaimer, the term of this patent is extended or adjusted under 35 U.S.C. 154(b) by 455 days.

(21) Appl. No.: **18/083,945**

(22) Filed: **Dec. 19, 2022**

(65) **Prior Publication Data**

US 2023/0184536 A1 Jun. 15, 2023

Related U.S. Application Data

(60) Continuation-in-part of application No. 17/236,901, filed on Apr. 21, 2021, now Pat. No. 11,530,910,
(Continued)

(51) **Int. Cl.**
G01B 9/02091 (2022.01)
A61B 1/00 (2006.01)
(Continued)

(52) **U.S. Cl.**
CPC ***G01B 9/02091*** (2013.01); ***A61B 1/0005*** (2013.01); ***A61B 1/0017*** (2013.01);
(Continued)

(58) **Field of Classification Search**
CPC G01B 9/02091; G01B 2290/65; G01B 9/02044; G01B 9/02069; A61B 1/0005;
(Continued)

(56) **References Cited**

U.S. PATENT DOCUMENTS

6,294,775 B1 9/2001 Seibel et al.
6,563,105 B2 * 5/2003 Seibel H04N 23/55 250/234
(Continued)

FOREIGN PATENT DOCUMENTS

AU 2002331723 B2 3/2007
CN 1310615 C 4/2007
(Continued)

OTHER PUBLICATIONS

U.S. Appl. No. 11/833,831, filed Aug. 3, 2007, Johnston et al.
(Continued)

Primary Examiner — Michael P LaPage
(74) *Attorney, Agent, or Firm* — BakerHostetler

(57) **ABSTRACT**

Methods for synchronizing an Optical Coherence Tomography (OCT) system including detection when a plurality of A-line scans obtained from reflected light of a cantilever scanning fiber within a probe oscillating along a scanning path that increases in amplitude over time are no longer being obtained at a point along the oscillating scanning path when the scanning fiber reaches a minimum speed, determining a value by which a phase angle of the oscillating scanning path is out of synchronization with the plurality of A-line scans, and adjusting a trigger clock for the obtaining the plurality of A-line scans based on the value.

14 Claims, 16 Drawing Sheets

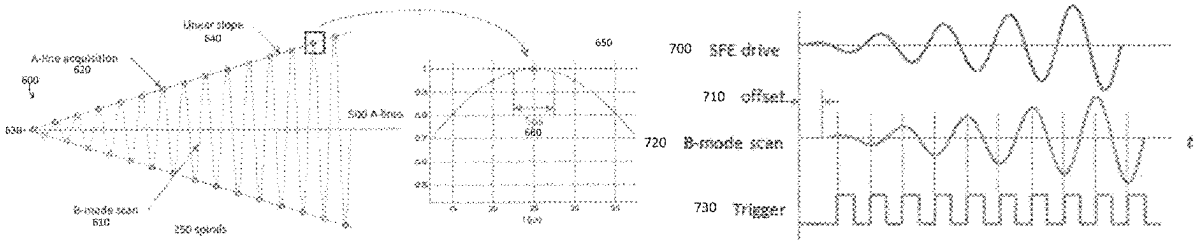

Related U.S. Application Data

which is a division of application No. 16/777,807, filed on Jan. 30, 2020, now Pat. No. 11,047,671.

(51) **Int. Cl.**

A61B 3/10	(2006.01)
A61B 5/00	(2006.01)
A61B 90/00	(2016.01)
G01B 9/02055	(2022.01)

(52) **U.S. Cl.**

CPC ***A61B 3/102*** (2013.01); ***A61B 5/0066*** (2013.01); *A61B 2090/3735* (2016.02); *G01B 9/02069* (2013.01); *G01B 2290/65* (2013.01)

(58) **Field of Classification Search**

CPC A61B 1/0017; A61B 3/102; A61B 2090/3735; A61B 3/1233; A61B 5/0066

See application file for complete search history.

(56) **References Cited**

U.S. PATENT DOCUMENTS

6,845,190	B1	1/2005	Smithwick et al.	
6,856,712	B2	2/2005	Fauver et al.	
6,959,130	B2	10/2005	Fauver et al.	
6,975,898	B2	12/2005	Seibel	
7,068,878	B2	6/2006	Crossman-Bosworth et al.	
7,159,782	B2	1/2007	Johnston et al.	
7,189,961	B2	3/2007	Johnston et al.	
7,252,236	B2	8/2007	Johnston et al.	
7,298,938	B2	11/2007	Johnston	
7,312,879	B2	12/2007	Johnston	
7,349,098	B2	3/2008	Li	
7,391,013	B2	6/2008	Johnston et al.	
7,395,967	B2	7/2008	Melville	
7,447,415	B2	11/2008	Melville et al.	
7,522,813	B1	4/2009	Johnston et al.	
7,583,872	B2	9/2009	Seibel et al.	
7,608,842	B2	10/2009	Johnston	
7,616,986	B2	11/2009	Seibel et al.	
7,680,373	B2	3/2010	Melville et al.	
7,738,762	B2	6/2010	Melville et al.	
7,784,697	B2	8/2010	Johnston et al.	
7,791,009	B2	9/2010	Johnston et al.	
7,813,538	B2	10/2010	Carroll et al.	
7,901,348	B2	3/2011	Soper et al.	
8,212,884	B2	7/2012	Seibel et al.	
8,305,432	B2	11/2012	Johnston	
8,382,662	B2	2/2013	Soper et al.	
8,411,922	B2	4/2013	Lee et al.	
8,437,587	B2	5/2013	Melville	
8,466,956	B2	6/2013	Sugimoto	
8,537,203	B2	9/2013	Seibel et al.	
8,840,566	B2	9/2014	Seibel et al.	
8,929,688	B2	1/2015	Johnston	
8,947,514	B2 *	2/2015	Shibasaki	H04N 23/74 348/65
8,957,484	B2	2/2015	Melville et al.	
9,066,651	B2	6/2015	Johnston	
9,160,945	B2	10/2015	Johnston	
9,226,687	B2	1/2016	Soper et al.	
9,554,729	B2	1/2017	Soper et al.	
9,561,078	B2	2/2017	Seibel et al.	
10,080,484	B2	9/2018	Yang et al.	
2001/0055462	A1	12/2001	Seibel	
2002/0064341	A1 *	5/2002	Fauver	G02B 6/3502 359/210.1
2002/0139920	A1	10/2002	Seibel et al.	
2005/0196324	A1 *	9/2005	Harris	A61B 5/0068 422/82.07
2006/0170930	A1	8/2006	Li	
2008/0058629	A1	3/2008	Seibel et al.	
2008/0144998	A1	6/2008	Melville et al.	
2008/0161648	A1	7/2008	Karasawa	
2008/0165360	A1	7/2008	Johnston	
2009/0028407	A1 *	1/2009	Seibel	A61B 1/0627 382/131
2009/0137893	A1	5/2009	Seibel et al.	
2013/0271757	A1	10/2013	Kang et al.	
2015/0159991	A1 *	6/2015	Hasegawa	G01B 9/02083 356/479
2018/0196250	A1	7/2018	Shimamoto	
2018/0256031	A1 *	9/2018	Adamson	G01B 9/02091
2018/0315194	A1	11/2018	Moult et al.	
2019/0223714	A1	7/2019	Raymond et al.	
2020/0273216	A1	8/2020	Kennedy et al.	
2021/0055543	A1	2/2021	Van Lierop et al.	
2021/0239451	A1	8/2021	McMorrow et al.	
2023/0128254	A1 *	4/2023	Hsu	G01N 21/39 356/479

FOREIGN PATENT DOCUMENTS

EP	1803008	A1	7/2007
EP	1805779	A1	7/2007
EP	1851673	A1	11/2007
EP	1954193	A1	8/2008
EP	2061367	A1	5/2009
EP	2096688	A2	9/2009
EP	2224841	A1	9/2010
EP	2225699	A1	9/2010
EP	1592992	B1	5/2012
EP	1691666	B1	5/2012
EP	2653995	A1	10/2013
EP	2179454	B1	1/2016
EP	2099353	B1	9/2018
EP	2092388	B1	10/2018
EP	3415075	A1	12/2018
EP	3552534	A2	10/2019
JP	4080426	B2	4/2008
JP	2009-212519	A	9/2009
JP	2011-504782	A	2/2011
JP	2011-504783	A	2/2011
JP	4672023	B2	4/2011
JP	5025877 82		9/2012
JP	5069105	B2	11/2012
JP	5069310	B2	11/2012
JP	5097270	B2	12/2012
JP	5190267 82		4/2013
JP	5513897	B2	6/2014
JP	5608718	B2	10/2014
JP	5781269	B2	9/2015
WO	WO 2001/097902	A2	12/2001
WO	WO 2003/019661	A1	3/2003
WO	WO 2004/068218	A2	8/2004
WO	WO 2005/058137	A2	6/2005
WO	WO 2006/004743	A2	1/2006
WO	WO 2006/041452	A1	4/2006
WO	WO 2006/041459	A1	4/2006
WO	WO 2006/071216	A1	7/2006
WO	WO 2006/096155	A1	9/2006
WO	WO 2007/067163	A1	6/2007
WO	WO 2007/106075	A2	9/2007
WO	WO 2008/033168	A1	3/2008
WO	WO 2008/076149	A1	6/2008
WO	WO 2008/085186	A1	7/2008
WO	WO 2009/014525	A1	1/2009
WO	WO 2009/070160	A1	6/2009
WO	WO 2009/070161	A1	6/2009
WO	WO 2019/071295	A1	4/2019

OTHER PUBLICATIONS

U.S. Appl. No. 60/138,404, filed Jun. 8, 1999, Seibel.
U.S. Appl. No. 60/212,411, filed Jun. 19, 2000, Seibel.
U.S. Appl. No. 60/253,445, filed Nov. 27, 2000, Seibel et al.
U.S. Appl. No. 60/333,421, filed Nov. 26, 2001, Seibel et al.
U.S. Appl. No. 60/442,852, filed Jan. 24, 2003, Seibel et al.
U.S. Appl. No. 60/529,077, filed Dec. 12, 2003, Seibel et al.
U.S. Appl. No. 60/644,335, filed Jan. 14, 2005, Li.
U.S. Appl. No. 60/912,237, filed Apr. 17, 2007, Carroll et al.

(56) **References Cited**

OTHER PUBLICATIONS

U.S. Appl. No. 61/589,069, filed Jan. 20, 2012, N/A.
U.S. Appl. No. 61/934,479, filed Jan. 31, 2014, Yang et al.
International Patent Application No. PCT/2021/14972; Invitation to Pay Add'l Fees; dated Mar. 9, 2021; 2 pages.
International Patent Application No. PCT/US2023/084141; Int'l Search Report and the Written Opinion; dated May 1, 2024; 7 pages.

* cited by examiner

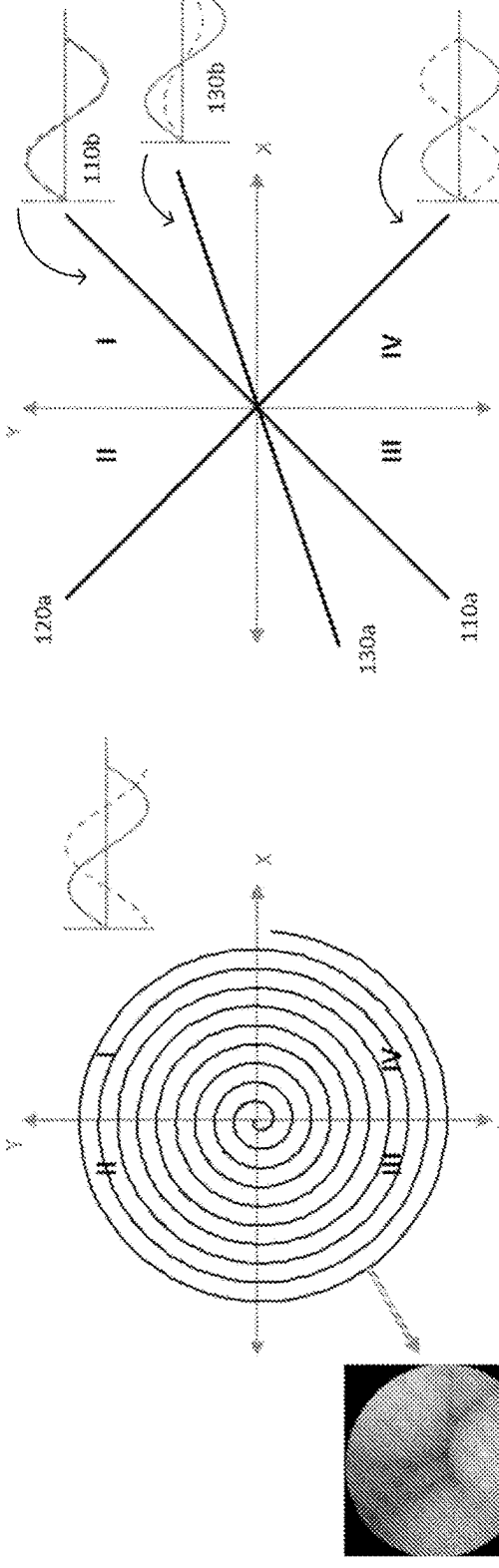

FIG. 1A
RGB Surface Scan

FIG. 1B
Penetrating Scan

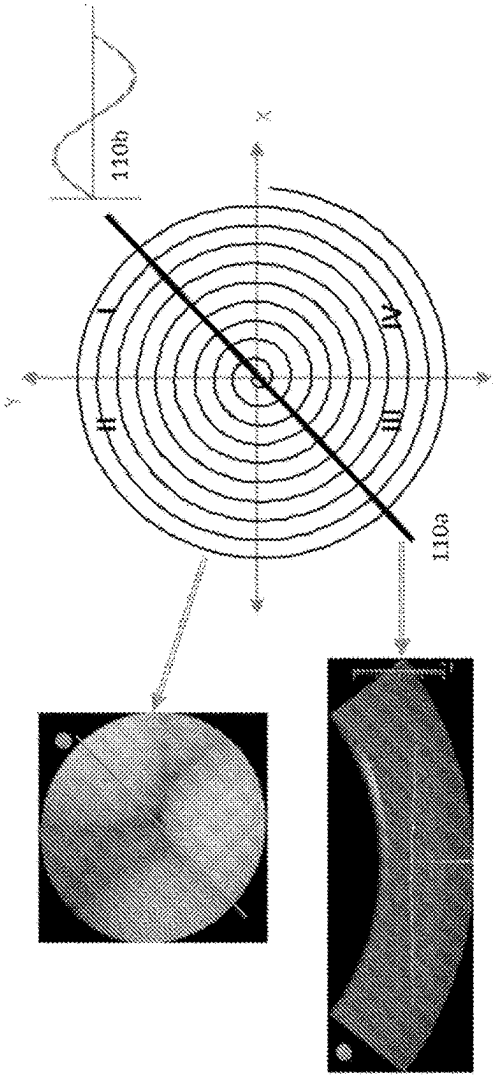

FIG. 1C
RGB Surface Scan and Penetrating Scan

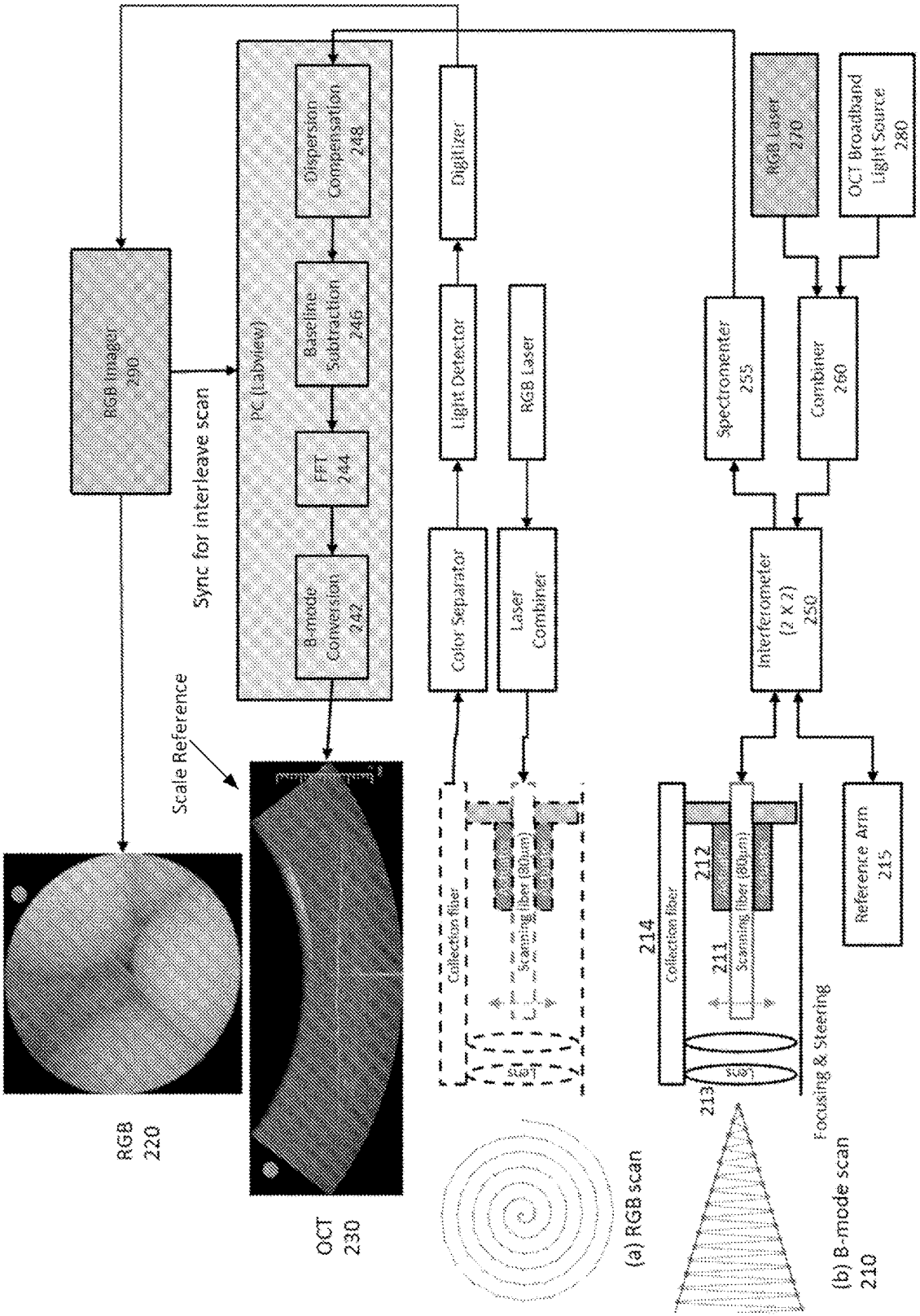
RGB Imager 290
Sync for interleave scan
PC (Labview)
Dispersion Compensation 248
Baseline Subtraction 246
FFT 244
B-mode Conversion 242
Digitizer
Light Detector
RGB Laser
Color Separator
Laser Combiner
Spectrometer 255
Combiner 260
RGB Laser 270
OCT Broadband Light Source 280
Interferometer (2 X 2) 250
Reference Arm 215
Scale Reference
RGB 220
OCT 230
Collection fiber
Scanning fiber (80μm)
214
212
211
213
Focusing & Steering
(a) RGB scan
(b) B-mode scan 210

FIG. 2

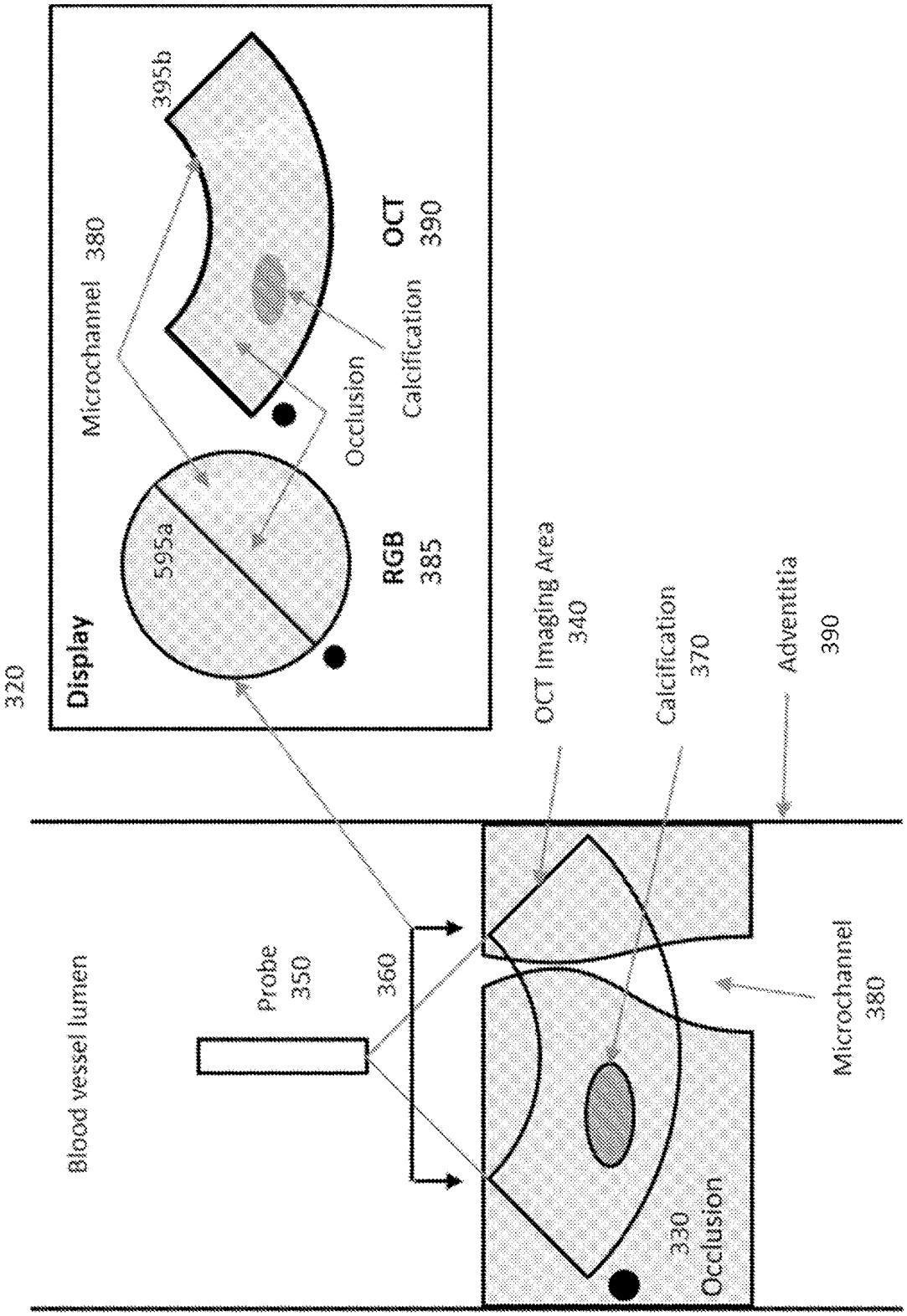
320
Display
595a
395b
Microchannel 380
Occlusion
Calcification
RGB 385
OCT 390
Blood vessel lumen
Probe 350
360
OCT Imaging Area 340
Calcification 370
Adventitia 390
330 Occlusion
Microchannel 380

FIG. 3

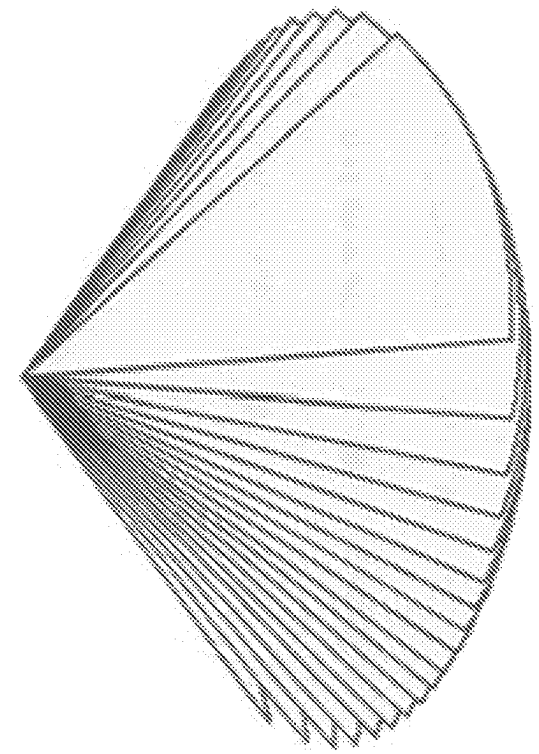

FIG. 4B

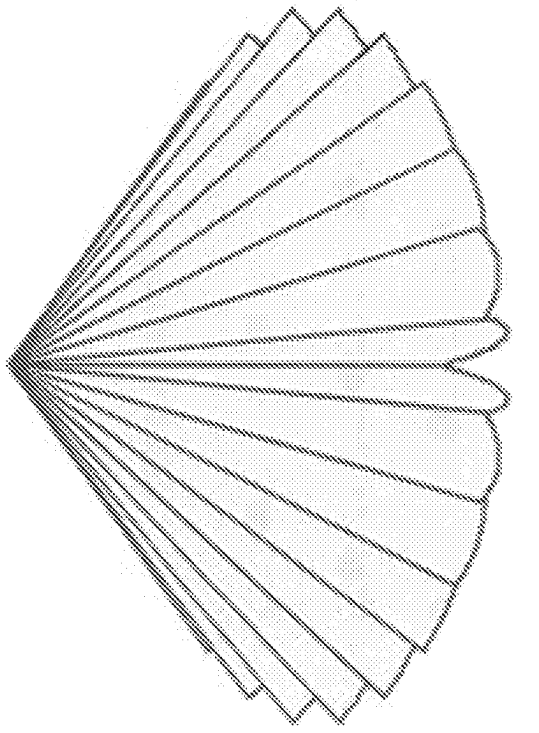

FIG. 4A

Simulated compounding image
FIG. 5B

Original OCT image
FIG. 5A

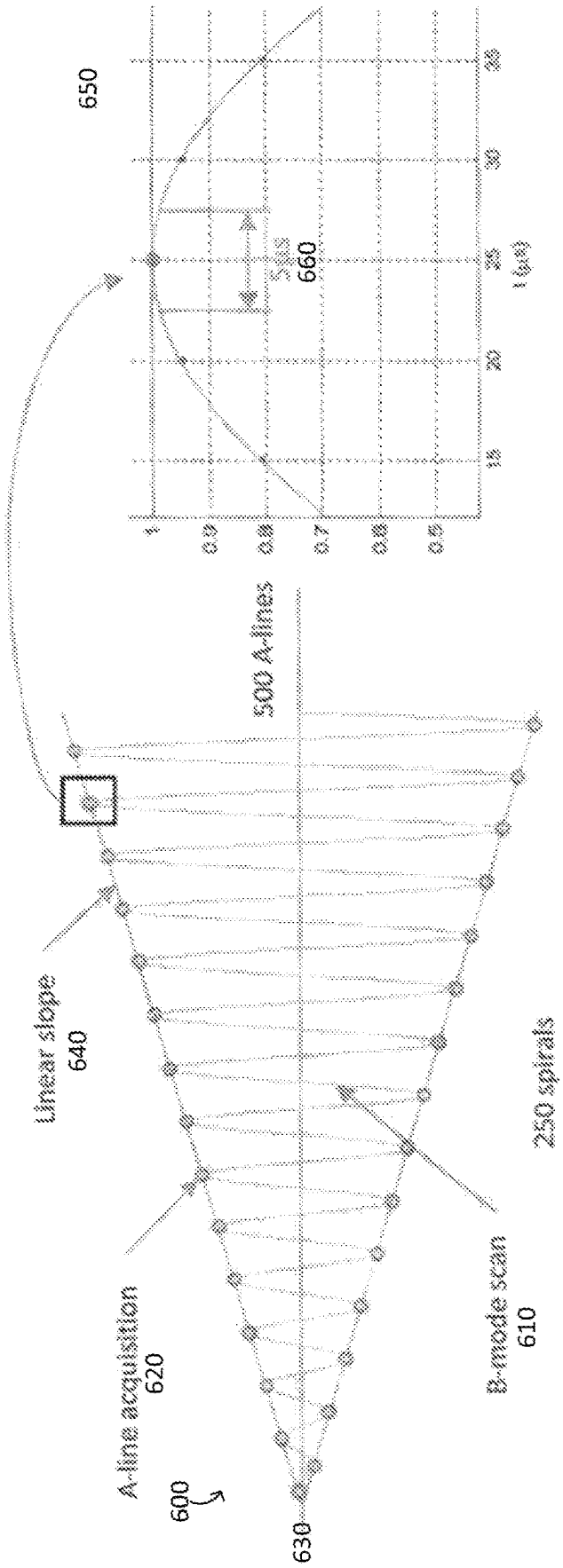
650
660
500 A-lines
Linear slope
640
250 spirals
A-line acquisition
620
B-mode scan
610
600
630

FIG. 6

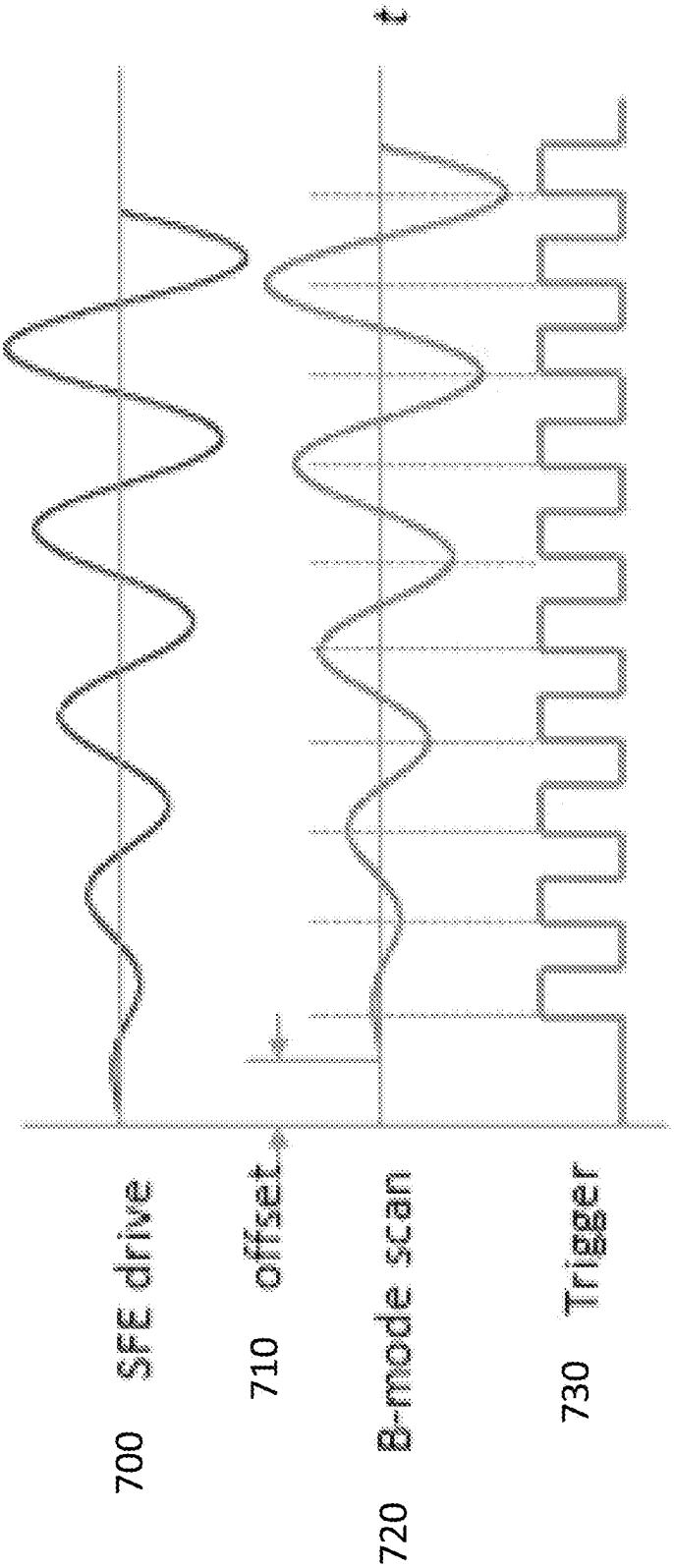

FIG. 7

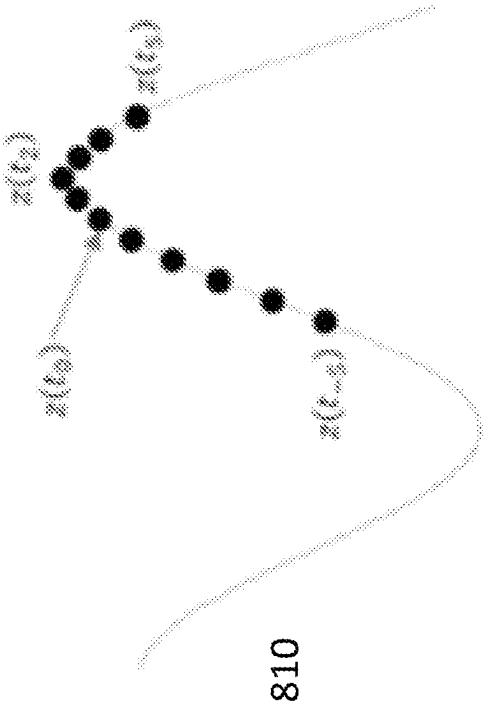

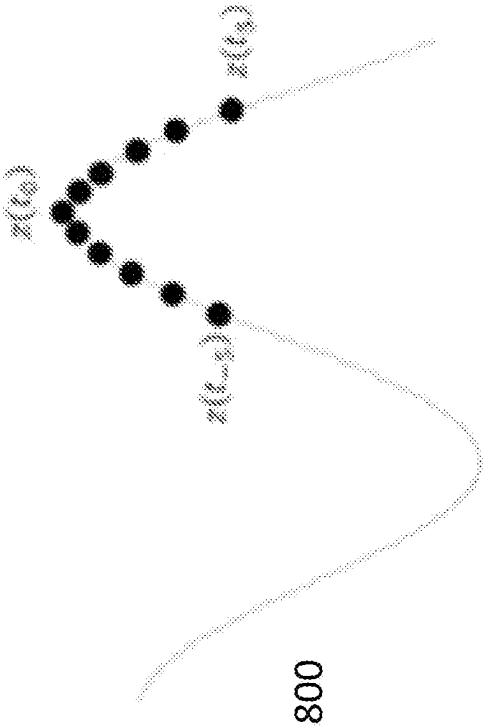

FIG. 8

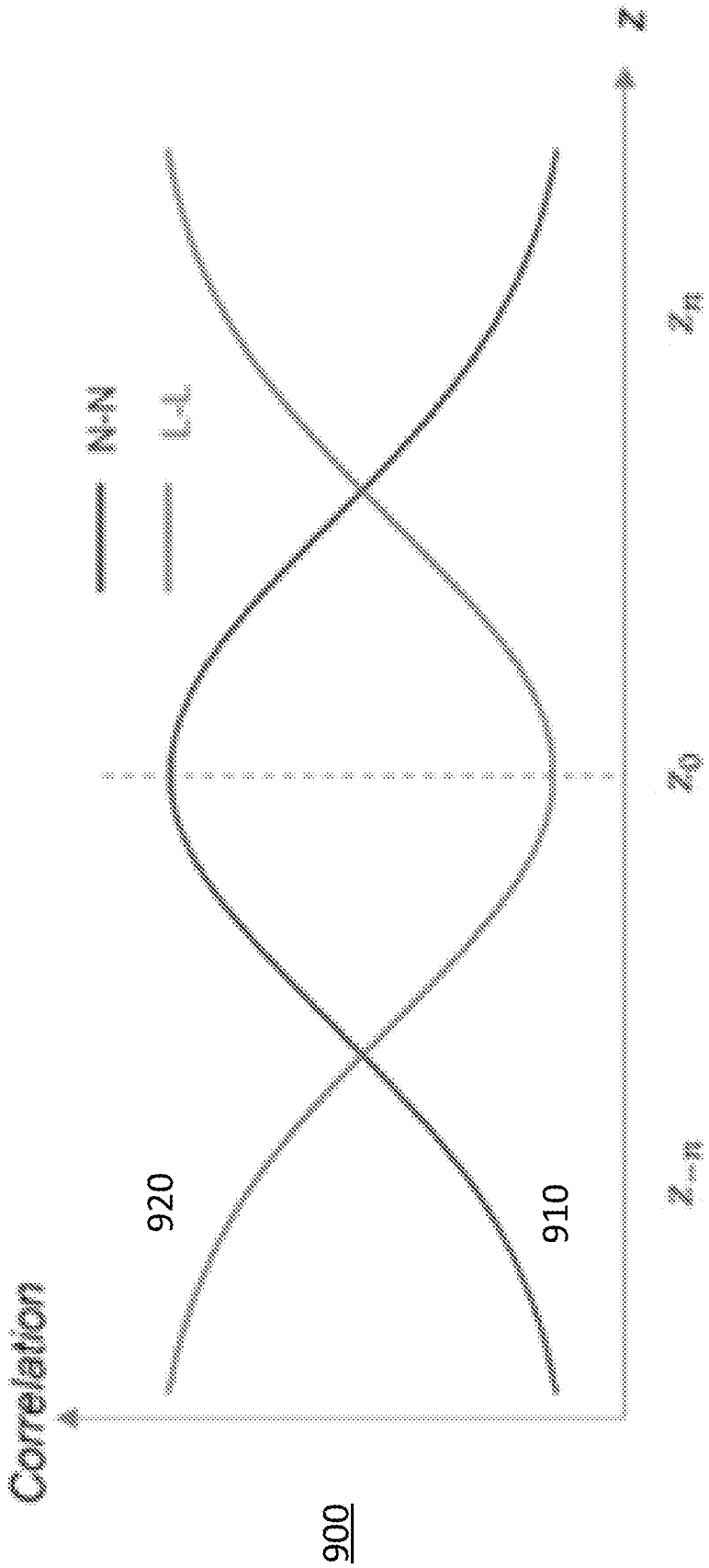

FIG. 9

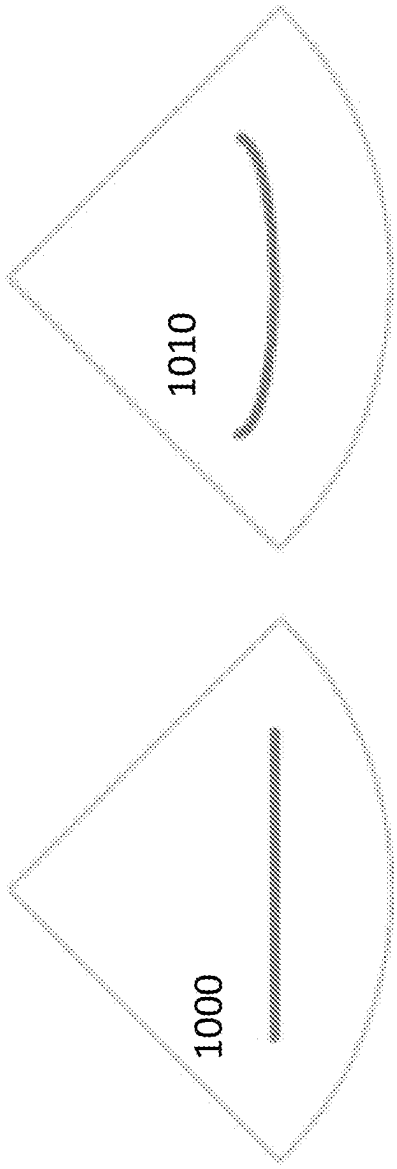

FIG. 10

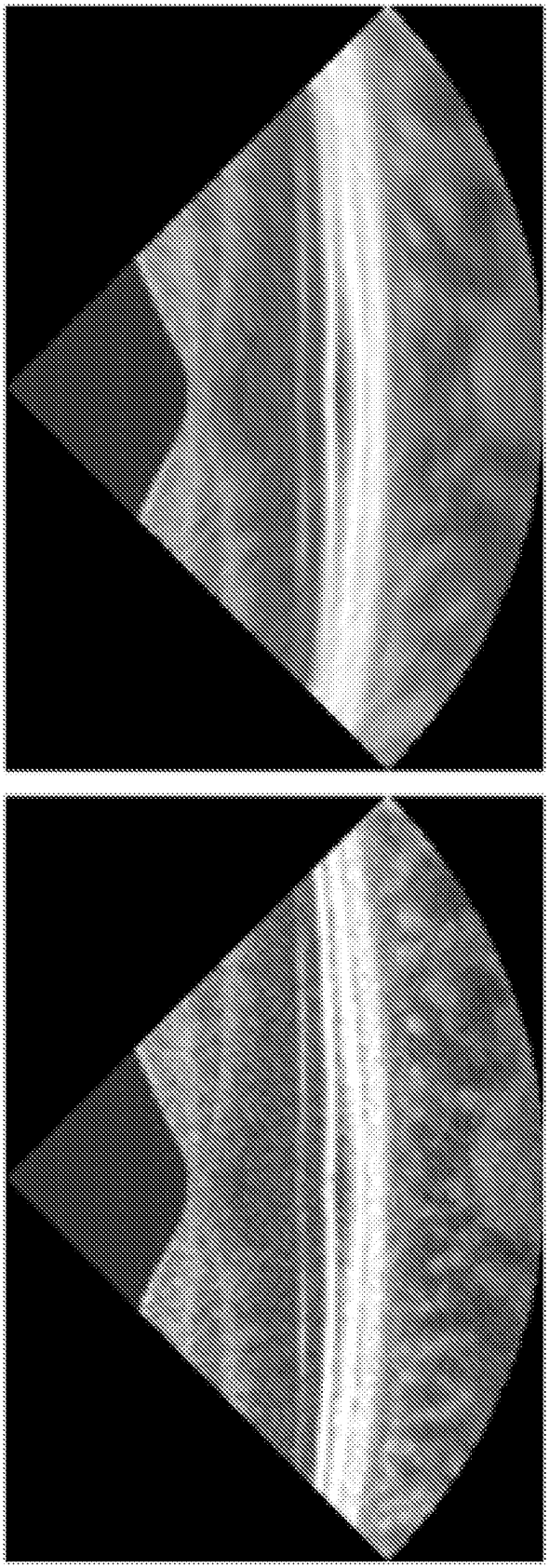

FIG. 11

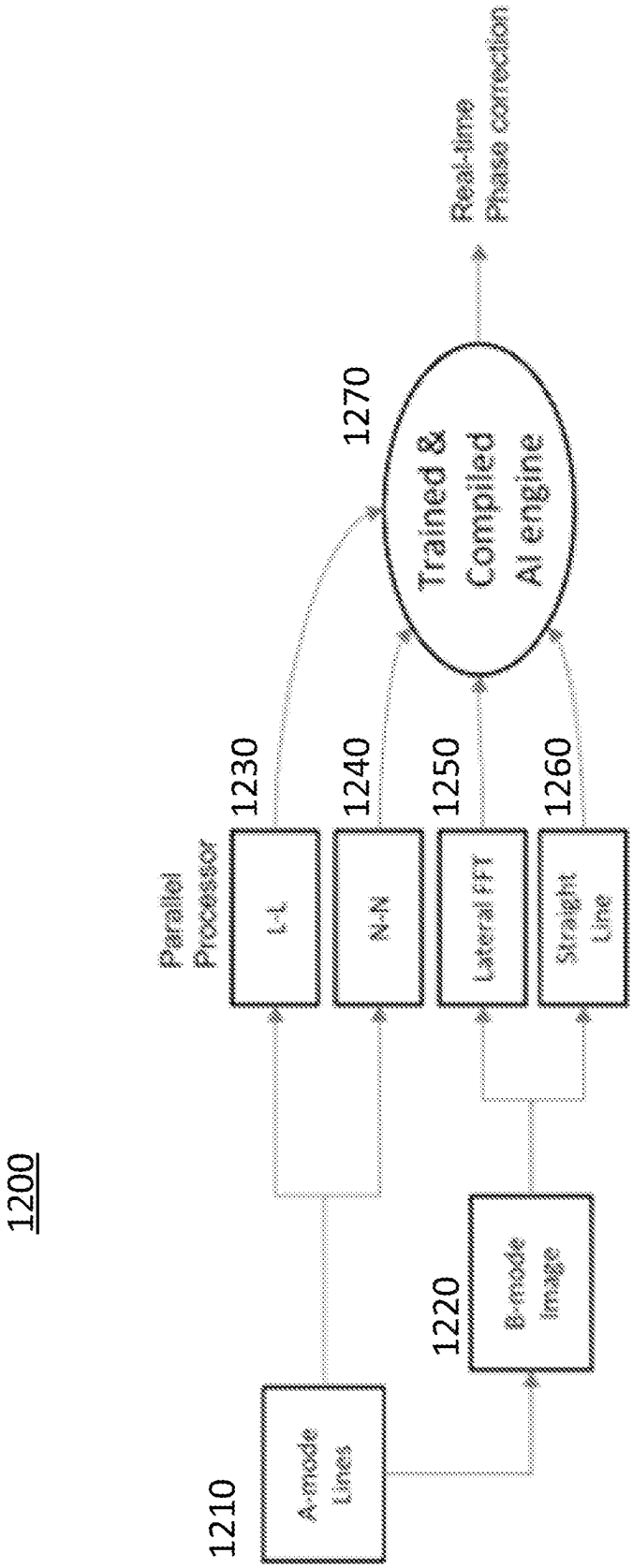
1200
1210
A-mode Lines
1220
B-mode Image
Parallel Processor
1230
1-1
1240
N-N
1250
Lateral FFT
1260
Straight Line
1270
Trained & Compiled AI engine
Real-time Phase correction

FIG. 12

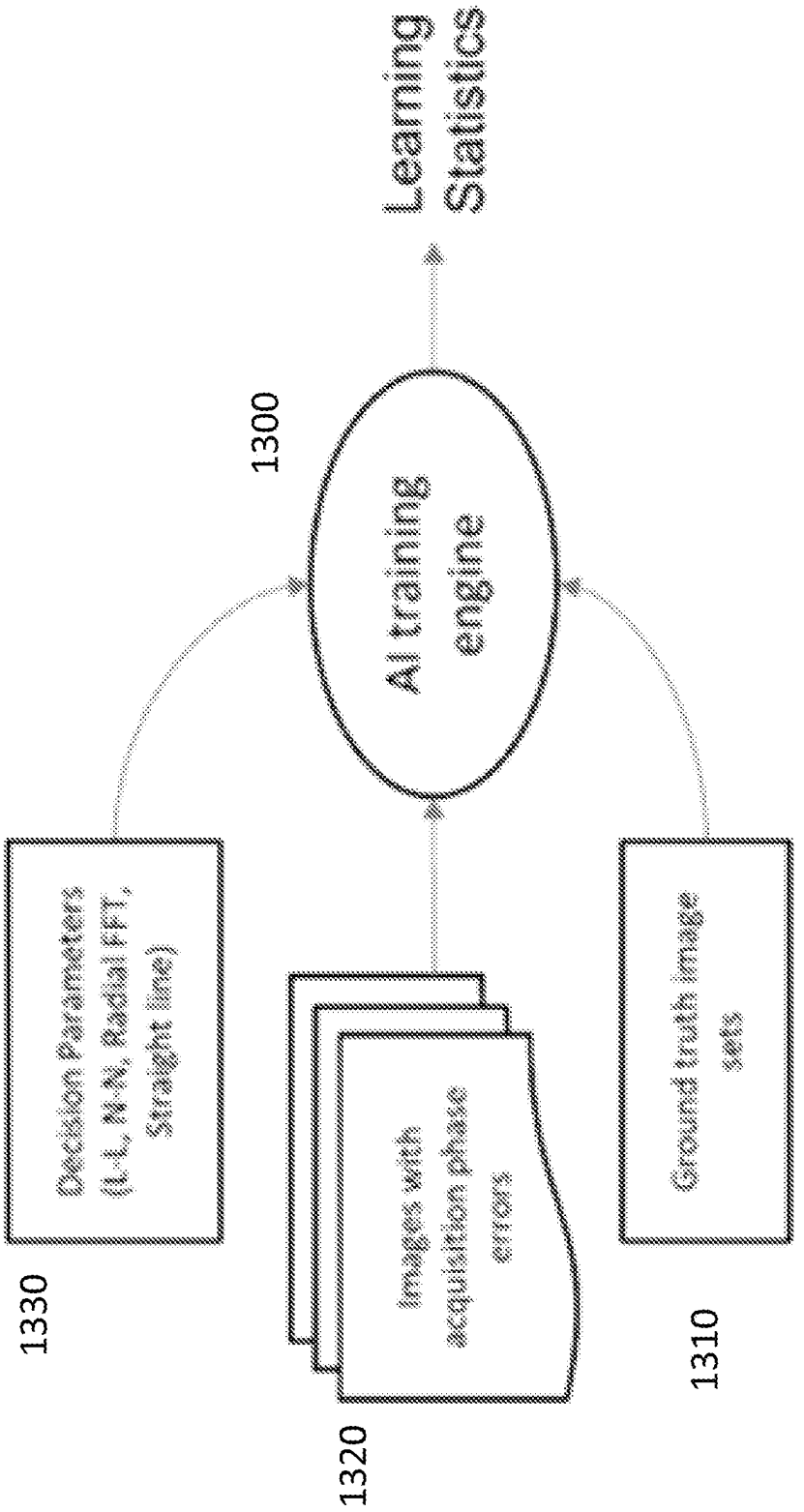
Learning Statistics
1300
AI training engine
Decision Parameters (I-L, M-N, Radial FFT, Straight line)
1330
Images with acquisition phase errors
1320
Ground truth image sets
1310

FIG. 13

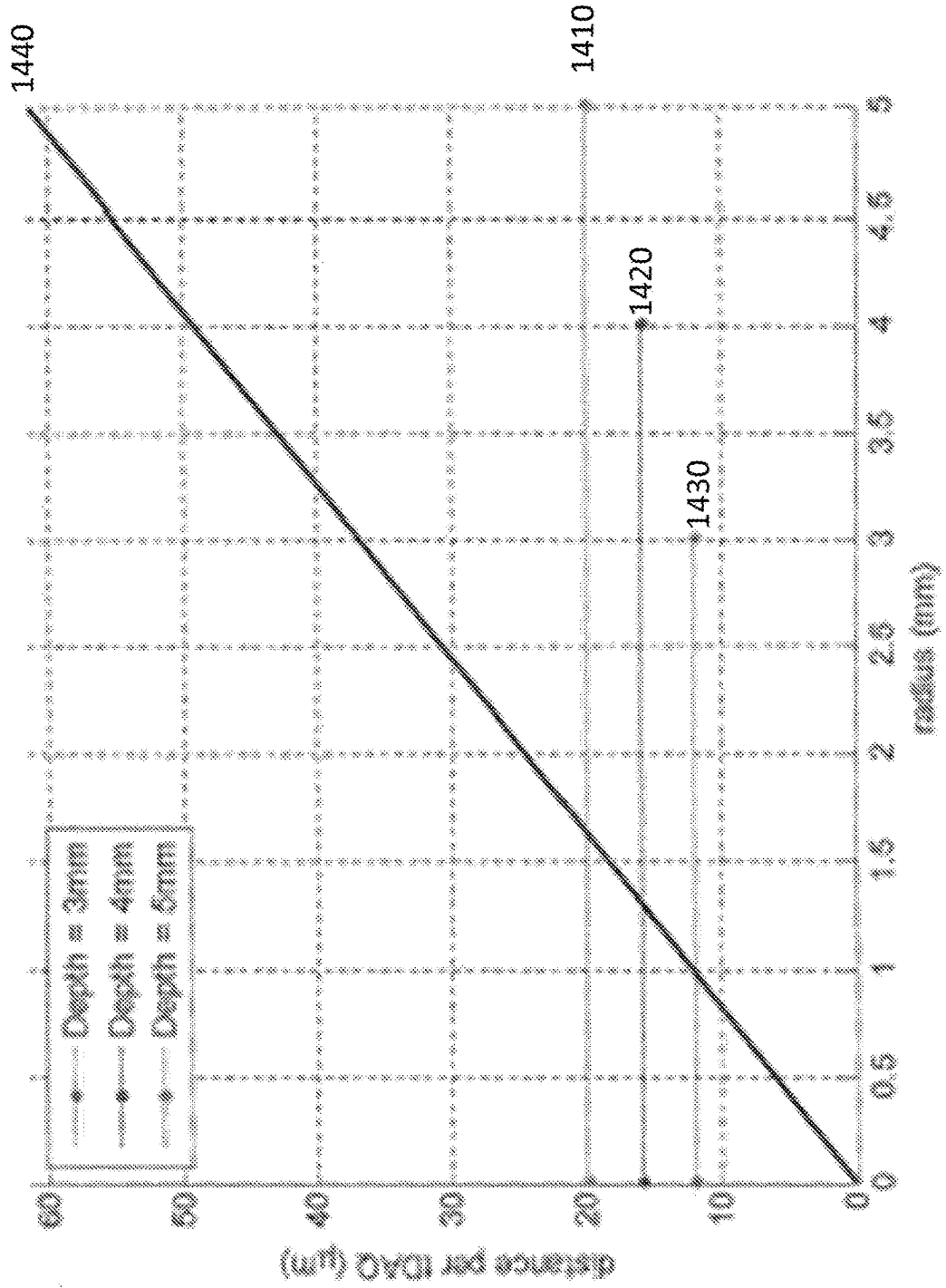
1440
1410
1420
1430
Depth = 3mm
Depth = 4mm
Depth = 5mm
distance per load (μm)
radius (mm)
0
10
20
30
40
50
60
70
0
0.5
1
1.5
2
2.5
3
3.5
4
4.5
5

FIG. 14

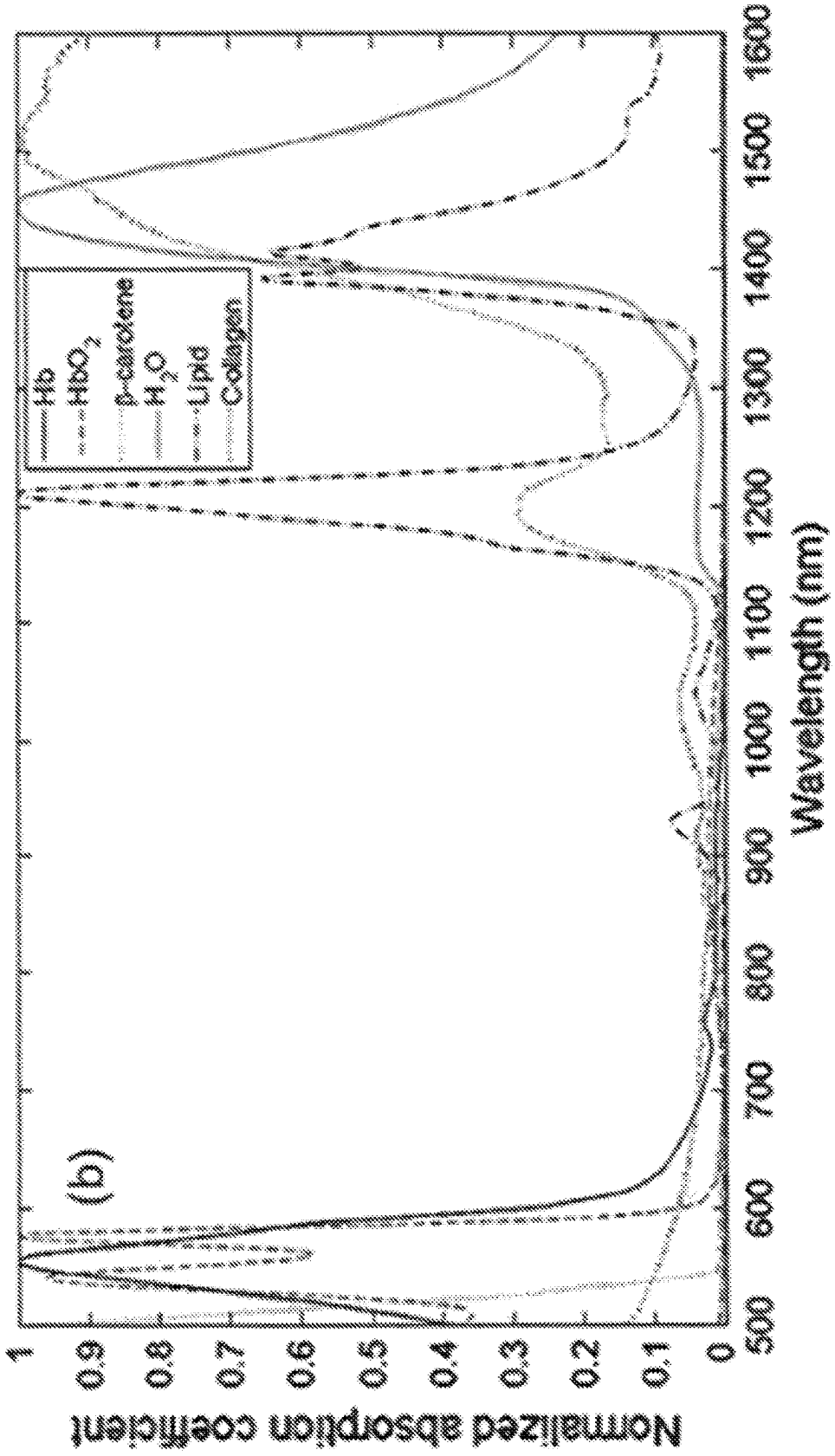
Normalized absorption coefficient
0
0.1
0.2
0.3
0.4
0.5
0.6
0.7
0.8
0.9
1
500
600
700
800
900
1000
1100
1200
1300
1400
1500
1600
Wavelength (nm)
(b)
Hb
HbO2
β-carotene
H2O
Lipid
Collagen

FIG. 15

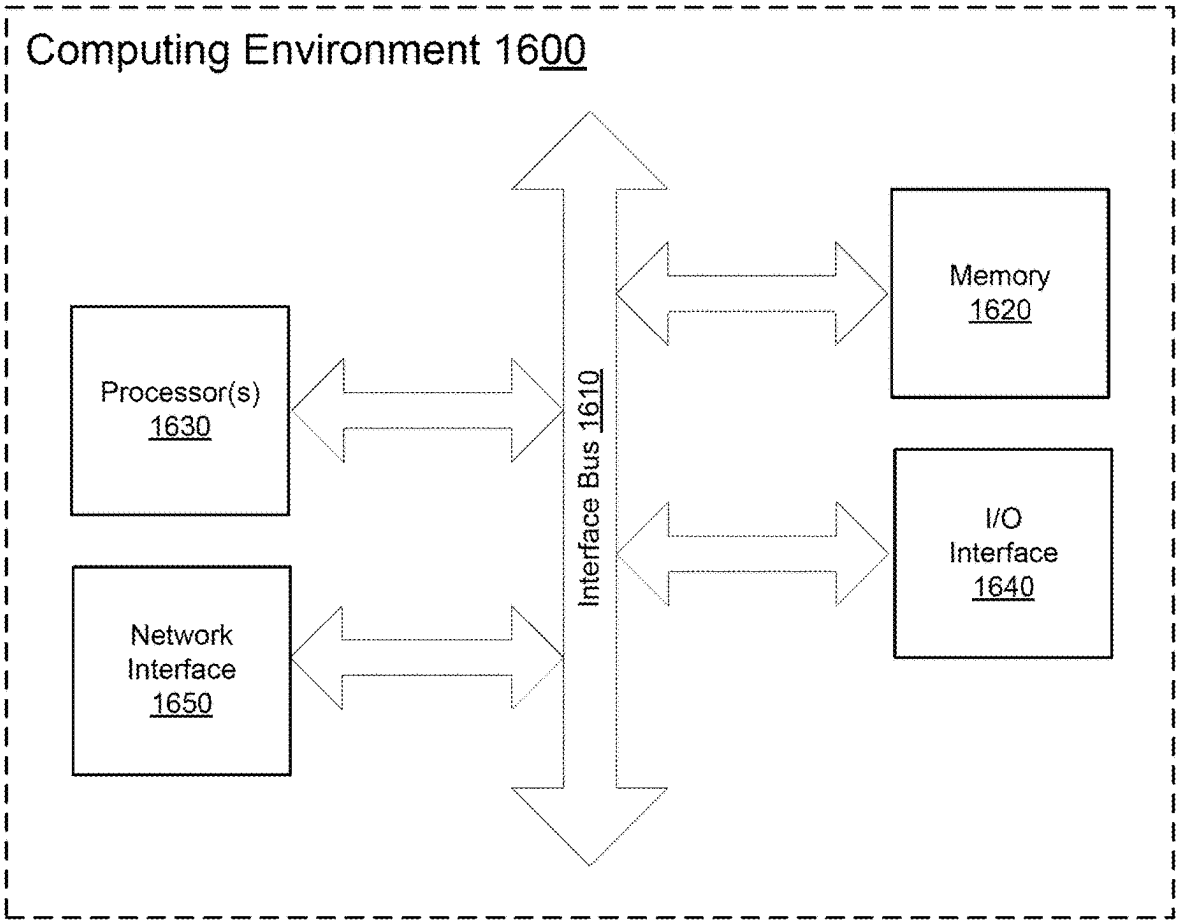
Computing Environment 1600
Interface Bus 1610
Memory 1620
Processor(s) 1630
I/O Interface 1640
Network Interface 1650

FIG. 16

SYNCHRONIZING AN OPTICAL COHERENCE TOMOGRAPHY SYSTEM

CROSS REFERENCE TO RELATED APPLICATIONS

This application is a continuation-in-part of U.S. patent application Ser. No. 17/236,901, filed Apr. 21, 2021, which is a divisional of U.S. patent application Ser. No. 16/777,807, filed Jan. 30, 2020, the contents of which is incorporated herein by reference in its entirety.

BACKGROUND

Chronic Total Occlusion (CTO) refers to a complete obstruction of the coronary artery. CTOs can result from coronary artery disease and develop due to atherosclerosis. The blockage prevents all downstream blood flow, and can cause a range of symptoms and issues, including chest pain and heart attacks. In some patients, however, CTOs cause no physically identifiable symptoms, e.g., silent heart attacks, and the CTOs go undiagnosed. Many patients with CTO also do not receive therapy due to practical difficulties of penetrating the occlusion with partially complete angiographic images.

Intravascular Ultrasound (IVUS) and Optical Coherence Tomography (OCT) are two current methods for intercoronary imaging. IVUS traditionally utilizes a catheter with an ultrasound probe on a proximal end and provides a cross-sectional view of blood vessels. OCT operates similarly but utilizes the longitudinal partial coherence of light rather than time delay of sound waves, to obtain information from reflected, scattered light. OCT can provide resolution on the order of micrometers, but its penetration depth is often limited to several millimeters below tissue surface. Both IVUS and OCT provide only a radial visualization at the imaging location. This requires the imaging device to pass by the occlusion to image it. When applied to arterial imaging and diagnosing CTO's, for example, these techniques can provide cross-sectional information of the vessel, such as, indications of narrowing in the artery, e.g., due to plaque build-up, but cannot provide information beyond the position of their side scanning sensors within the vessel. Therefore, when a CTO or other blockage is present, current IVUS and OCT probes must penetrate the occlusion before any CTO visualization is possible.

Penetration of the occlusion is often the blocking step to being able to complete therapy such as placing a stent. Penetration with a guidewire, for example, can be very time-consuming, e.g., 30 minutes or more, and in some cases, penetration is not possible. Accidentally exiting the lumen with the guidewire poses an additional risk, as doing so can cause significant damage to the patient. As such, it would be advantageous to have the ability to identify and visualize an occlusion prior to and during the penetration procedure.

Scanning Fiber Endoscopes (SFE) can provide color imaging based on RGB reflectance, and wide-field viewing of the internal arterial region and proximal CTO. SFE imaging techniques only provide surface information within the artery and of the proximal end of the CTO. The invention herein combines forward looking RGB reflectance images combined with forward penetrating sectional images of CTO using OCT.

SFE probes scan at approximately 10 kHz for RGB imaging, which provides a single revolution time of about 100 μs. This rotation leaves little time for any OCT scan.

Scanning with OCT while changing the location of the scan this quickly would cause the OCT image to be useless from excessive lateral motion artifact. OCT imagers require 7-8 us imaging time per line and deliver a 100 kHz A-line acquisition speed. At this rate, during one spiral rotation, only 10 A-line samples can be obtained, thus resulting in poor OCT lateral resolution due to probe movement artifact during the wavelength-sweep and a lack of A-lines to compose the penetrating B-mode image. To reduce the rotational speed of the SFE probe, significant modifications are required to be made, e.g., changing the length of fiber inside the SFE, but such changes are often not adequate for RGB imaging, causing slow frame rates and larger rigid length of the RGB imager.

SUMMARY

Methods for synchronizing an Optical Coherence Tomography (OCT) system is disclosed including detection when a plurality of A-line scans obtained from reflected light of a cantilever scanning fiber within a probe oscillating along a scanning path that increases in amplitude over time are no longer being obtained at a point along the oscillating scanning path when the scanning fiber reaches a minimum speed, determining a value by which a phase angle of the oscillating scanning path is out of synchronization with the plurality of A-line scans, and adjusting a trigger clock for the obtaining the plurality of A-line scans based on the value.

As discussed herein, the present invention can be applied to various medical applications, including but not limited to scanning and imaging within a blood vessel lumen to identify at least one of an occlusion, a defect within an occlusion, a calcification, adventitia, a microchannel, or other features within a vessel or the body.

BRIEF DESCRIPTION OF THE DRAWINGS

The combination of the two imaging modalities and other features of the present disclosure will become more fully apparent from the following description and appended claims, taken in conjunction with the accompanying drawings. Understanding that these drawings depict only several examples in accordance with the disclosure and are, therefore, not to be considered limiting of its scope, the disclosure will be described with additional specificity and detail through use of the accompanying drawings.

In the drawings:

FIG. **1**(*a*) illustrates a forward looking SFE image with an RGB image of a human finger shown in the inset.

FIG. **1**(*b*) illustrates several line scans where, using methods described herein, OCT penetrating image of a cross-sectional "cutaway image" can be displayed. Thus, the system herein can scan with a spiral raster scan or can scan with line scans as shown in FIG. **1**(*b*).

FIG. **1**(*c*) illustrates a cross-sectional image plane that can be selected electronically relative to the RGB surface image.

FIG. **2** illustrates a block diagram of a duplex imager capable of RGB surface images and OCT penetrating images in accordance with embodiments described herein.

FIG. **3** illustrates a duplex image system inserted into a lumen **310**. Display **320** illustrates duplex imager having RGB surface image and OCT penetrating image of a CTO **330**.

FIGS. **4**(*a*) and **4**(*b*) illustrate two methods of constructing three-dimensional images from the OCT penetrating image

frames, with FIG. **4**(*a*) illustrating a method using acquired planes, and FIG. **4**(*b*) illustrating a method using reconstructed slices.

FIG. **5**(*a*) illustrates a normal, slowly scanned OCT image and FIG. **5**(*b*) illustrates a simulated compounding image

FIG. **6** illustrates the critical method to scan and acquire the OCT mode penetrating scan, during one frame of normal use for a surface RGB image.

FIG. **7** illustrates the synchronization of a spectrometer trigger clock with the driving frequency of an SFE probe.

FIG. **8** illustrates a correlation-based synchronization scheme for synchronization using OCT A-mode scans/samples collected while the SFE probe sweeps the object at the edge.

FIG. **9** illustrates a correlation plot for Line-to-Line and Neighbor-to-Neighbor correlations.

FIG. **10** illustrates a B-mode scan of a flat surface for use in a flat-surface imaging synchronization scheme.

FIG. **11** illustrates the relationship between synchronized and un-synchronized B-mode scans related to image focus for an image focus-based synchronization scheme.

FIG. **12** is a block diagram illustrating a processing implementation of the various synchronization schemes.

FIG. **13** is a block diagram illustrating a scheme for training the AI engine of FIG. **12**.

FIG. **14** illustrates a relationship between lateral resolution and a radius of a B-mode scan.

FIG. **15** illustrates absorption coefficients of tissue constituents for various wavelengths.

FIG. **16** illustrates an example computing environment in accordance with embodiments discussed herein.

DETAILED DESCRIPTION OF ILLUSTRATIVE EMBODIMENTS

In the following detailed description, reference is made to the accompanying drawings, which form a part hereof. In the drawings, similar symbols typically identify similar components, unless context dictates otherwise. The illustrative examples described in the detailed description, drawings, and claims are not meant to be limiting. Other examples may be utilized, and other changes may be made, without departing from the spirit or scope of the subject matter presented here. It will be readily understood that the aspects of the present disclosure, as generally described herein, and illustrated in the Figures, may be arranged, substituted, combined, and designed in a wide variety of different configurations, all of which are explicitly contemplated and make part of the present disclosure.

The present disclosure relates to duplex imaging techniques. More particularly, the present disclosure combines high-resolution surface images obtained with SFE, and high-resolution penetrating OCT images obtained through Optical Coherence Tomography (OCT), from a Scanning Fiber Endoscope (SFE), and interleaving frames to improve resolution and identify below surface information of biological structures. As applied to CTOs, SFE high resolution color imaging technology combined with forward-looking OCT, allows visualization of occlusions, and visualization below the surface of the occlusion prior to penetration. In addition, micro channels, calcifications, and adventitia can be imaged to provide additional clinical benefits and information. With the forward-looking imaging, a physician can, for example, identify and more safely penetrate the CTO, using a guidewire or other means, and identify a CTO's location and strong or weak aspects (calcification or microchannels) prior to penetration. Aspects of the invention further provide the ability to acquire three-dimensional (3D) OCT data. Thus, combining SFE and interleaved frames of an OCT can provide a forward viewing direction and cross-sectional information of the CTO.

The present invention can utilize certain OCT A-line acquisitions to construct frames of compounded B-mode images to identify a subsurface tissue information. FIG. **1**(*b*), for example, identifies possible B-mode scanning angles, as indicated on a Cartesian plane with the straight lines, each input can be represented by a sinusoidal wave, and the phase difference between the inputs control the motion of imaging scans, which are typically linear. Note that OCT images are gathered only when the linear scan reaches the maximum amplitude and minimum velocity, this allows excellent OCT lateral resolution. This slow motion is like the momentary lack of motion when a child's swing reaches max height and reverses direction.

There are also frames of spiral surface mode scans depicted in FIG. **1**. These form a raster scan to scan the surface of the scene in front of it. Note that the surface speed of the scanning is very high and would "smear" the OCT scans, thus the spiral scan is used for OCT only.

Moreover, by combining B-mode scans from various rotational angles, a cone-shaped three-dimensional image can be obtained. The 3D data can be visualized in the form of multiple B-mode images acquired or reconstructed from various directions and angles.

FIG. **1**(*b*) illustrates these principles and B-mode scanning angles with respect to a cartesian coordinate plane. Based on the relative angles between two inputs (X and Y) to the OCT probe, the overall probe motion will vary. The cartesian plane and lines **110**, **120**, **130** (as more fully described herein) are indicative of the probe's scanning angle with respect to a top surface of an OCT image. In other words, the two inputs X and Y represent an oscillating movement of the probe with respect to the imaging plane. The relationship between X and Y indicates the overall scanning motion, which can result in imaging of a particular area in a potential OCT field of view.

In a first example, FIG. **1**(*a*) illustrates a forward looking SFE image of the surfaces of the anatomy facing the imaging SFE catheter. A spiral raster scan may be used to bend the SFE fiber using a cantilever resonance of the fiber stub within the SFE imager. An RGB image of a human finger, as an example of the anatomy that can be imaged, from an actual imager is shown in the inset. In the spiral surface scan mode of FIG. **1**(*a*), two orthogonal sinusoidal waves, X and Y, with the same frequency, e.g., sin ($2\pi ft$) and cos ($2\pi ft$), can create a circular motion for imaging if the phase differences of the sinusoidal waves are 90° or $\pi/2$ radians.

In another example shown in FIG. **1**(*b*), OCT Penetrating Scan Mode **110***a*, the phase difference is 0°, i.e., the phase for each input is the same, then the circular motion becomes a linear motion, as illustrated by line **110***a* in Quadrants I and III, and the corresponding graph **110***b* when X=Y. The angle is controlled via relative amplitude. The **130***a* and **110***a* scans differ only in amplitude, same phase.

In another example shown in FIG. **1**(*b*), OCT Penetrating Scan Mode **120***a*, a phase difference of 180° or π radians between each input, X and Y, also results in the scanning motion becoming linear, as represented by line **120***a* in Quadrants II and IV, and corresponding graph **120***b*. In particular, graph **120***b* illustrates a relationship wherein X=−Y. Here, similar to the example of line **110***a* and graph **110***b*, the scanning motion is linear, but in the opposite

direction and in opposite Quadrants. Scan angles are controlled by amplitude; the same phase shown is equal amplitudes.

FIG. **1**(*c*) illustrates one such cross-sectional image plane that can be selected electronically relative to the RGB surface image, with the various scanning angles graphed on a Cartesian plane. The straight lines depict planes of penetrating OCT images that are possible, the spiral depicts the raster scan for the RGB surface image. These two image modalities occur by sharing frames in the 30 frame per second system disclosed herein. In effect one can have the RGB image and several planes of OCT "into the occlusion" images simultaneously. One could have 28 frames of RGB and 2 separate OCT "cutaway" images per second. The resultant user image pair is illustrated in the insets.

FIG. **2** illustrates a block diagram of an example duplex imaging system **200** usable with one or more embodiments discussed herein. The diagram illustrates a scanning probe **202**, such as an SFE, alternately performing both RGB scans **205** and penetrating B-mode scans **210**, along the linear line indicated on the RGB image **220**. The B-mode scan **210** along the linear line comprises collecting a plurality of A-mode information obtained at the oscillation endpoints of the scan (See also FIG. **6**). The collected information from the B-mode scan may be processed through one or more computing devices (e.g., PC **240**), interferometers (e.g., interferometer **250**), and spectrometers (e.g., spectrometer **255**) to produce the OCT image **230**. The RGB scan **205** produces the RGB surface image **220**, which is created from RGB reflected light through the collection fiber **214** of the scanning probe **202**. The RGB surface image is processed by color separator **223**, light detector **224**, and digitizer **225** and input to the RGB imager **290**.

A plurality of OCT images obtained from linear scans taken at various angles at the imaging location can be used to produce, a three-dimensional image, and/or information related to a forward-facing view from the end of the SFE.

In examples, surface-mode scans may be obtained from a spiral scanning fiber. As illustrated in FIG. **2**, the scanning probe **202** may comprise an oscillating scanning fiber **211** activated by one or more actuators **212**, one or more lenses **213** through which emitted light may be directed and focused, and the collection fiber **214** to receive reflected light for analysis. RGB light is able to propagate through the interferometer unaffected.

In OCT mode, the collected light may be first analyzed by at least one interferometer **250**, which can help identify an origin and location of reflected light. In embodiments, a reference arm **215** may be utilized to provide a reference point for the interferometer **250**, and additional components/systems such as an RGB laser **270**, OCT Broadband Light Source **280**, and combiner **260** can further contribute towards the interferometer's function.

From there, interferometer data, and additional spectrometer **255** data may be passed to the computing system **240**, which may comprise one or more computing devices to perform additional processing with regard to each obtained OCT image. Processing at PC **240** may comprise a B-mode conversion module **242**, Fast Fourier Transforms (FFT) **244**, a baseline subtraction module **246** and a dispersion compensation **248**. This processing can produce an OCT image **230**.

FIG. **3** illustrates an example imaging operation within a blood vessel which may utilize the B-Mode imaging system **200**. FIG. **3** illustrates a side view of a blood vessel lumen **310** containing an occlusion **330**, an OCT scanning/imaging area **340**, RGB scanned surface **360**, and a display **320** of the RGB SFE and OCT scanned area. A scanning probe **350**, which may comprise an oscillating scanning fiber as described herein, scans between width **360** to provide a forward-looking view within the blood vessel. As discussed herein, this forward view, e.g., along the length of the lumen, of the RGB image **360** and the penetrating view of **340** can allow observation of the surface of an occlusion **385** and a penetrating view of the occlusion **390** prior to or during contact or penetration.

In the present example, the occlusion **330** contains a calcification **370** and a microchannel **380** running through the occlusion. These features may be identified in the display section **320**, which illustrates an RGB surface image **385** and a corresponding penetrating OCT image **390** along a scanning line **395***a*. The OCT image **390** may permit observation of a first view of the occlusion **330** which likely depicts subsurface microchannel **380** as well as the calcification **370**. The RGB image **385** permits a surface view of the occlusion **385**. In other words, RGB images **385** combined with OCT subsurface images **390** are forward-facing and can therefore characterize and guide therapy upon occlusion **330** and other surface and subsurface features, e.g., microchannel **380**, within the viewable area in a manner not possible with either image alone.

OCT subsurface images are be obtained from a linear scanning motion. Each linear scan produces a fan-shaped OCT image **390**, which can provide depth information, and be usable to identify one or more features beyond or within occlusions, blockages, and areas beyond surface-level features. The resulting B-mode image targets comprise a plurality of A-lines orthogonal to the scanning path and typically have a fan shape since the origin of the scanning probe **350** and its light point is a single point oscillating between width **360**. The imaging depth in the fan-shaped B-mode can be determined by one or more variables in the OCT scanning scheme, including but not limited to reference arm length, swept-source bandwidth, and wavelength resolution.

Multiple linear penetrating OCT scans may be obtained at various angles across the circular RGB image scanning area. For example, the illustrated linear scan line **395***a* corresponds to the end view of the image plane of OCT image **390**. The scans along line **395***a* produce OCT image **390**, which may contain information indicative of the occlusion **330**, calcification **370**, and microchannel **380**. Subsequent linear scans may be obtained at the operator's command to the software, with each scan line being rotated around a central point in the viewing area **360**.

By composing the scanning patterns from various angles, three-dimensional images can be acquired. For example, using the various angles, i.e., 0° to 180°, and scanning at intervals. If 15° intervals are utilized, for example, twelve image planes can be obtained. FIG. **4**(*a*) illustrates this concept by generating three-dimensional data from a plurality of acquired linear planes. Since each obtained A-line information contains information along the light source path, the image has path-dependency. That is, the images are affected by the reflection of layers on the line of sight, and such data provides information to identify the object structure from the image. In medical applications, for example the three-dimensional object structure can provide valuable information to a clinician, such as volume of a region. Additionally, a volumetric survey of the CTO can be performed to allow the interventionalist to select the optimum crossing technique.

In another example, illustrated in FIG. **4**(*b*), two-dimensional image slices having path-dependency can be reconstructed to acquire the three-dimensional structure. The

sliced B-mode images can be obtained from an arbitrary scanning angle from the scan origin. In this way, path-dependency between slices can be preserved.

FIG. **5**(*a*) and FIG. **5**(*b*) illustrate results of the above recursive acquisition simulation. FIG. **5**(*a*) illustrates an original OCT B-mode image, wherein the image is slowly acquired using conventional OCT. FIG. **5**(*b*) is a simulated compounding image reconstructed using recursive data acquisition. The image dithering in FIG. **5**(*b*) is due to the simulated scanner translation during an OCT wavelength-sweep. In both images, the interval between A-lines are a 10-pixel distance.

FIG. **6** illustrates a B-mode edge scan and data acquisition scheme. The sinusoidal scanning path **600** represents the area through which a probe and its light source are driven during a linear scan. During a B-mode scan, the speed of the probe is at a maximum along center line **630**, and at a minimum (i.e., zero speed) along the edge line **620** (during which A-line acquisition occurs), which has an increasing, linear slope **640**. Note the slow scan motion during acquisition (i.e., 5 μSec).

In OCT scans, a slowly moving scan position during A-line acquisitions avoids distortions and smearing effects. Accordingly, in the current method, A-line data is exclusively collected at the endpoints of the B-mode scan, where the fiber scan movement is slowest while it reverses course. In this manner, data can be acquired at the most stable probe position.

The present example of FIG. **6** illustrates **250** oscillations or spirals, during the OCT B-mode scan **610** resulting in **500** A-line acquisitions along endpoints of the scanning area. In OCT B-mode scans, the radius is linearly increased as the scan travels along linear slope **640**. Graph **650** enlarges a portion of an edge lie scan at a point where the A-line data is collected, and the probe movement is minimal. In an example, a conventional spectral domain OCT can take 5 μs to take an A-line spectrometer reading **660**.

In embodiments of the OCT system, the spectrometer trigger clock (typically around 20 kHz) may be synchronized to the driving frequency of the SFE probe (typically around 10 kHz and half that of the trigger clock), along with a phase offset (a delay within a period (e.g., 50 μs)), in order to acquire two A-modes of data per a period of sinusoid at the edge of the B-mode scan. This is illustrated in FIG. **7**, where the driving frequency **700** is offset by an amount **710** so that an edge of the B-mode scan **720** is synchronized with the spectrometer trigger clock **730**, or vice versa.

The SFE probe is typically calibrated in a factory prior to delivery to an end user, but environmental conditions during subsequent use, such as aging or ambient temperature, can affect the driving pattern and phase and result in the spectrometer trigger clock no longer being synchronized to the edge of the B-mode scan. In embodiments, there may be at least three schemes for synchronizing the B-mode scan with the spectrometer trigger clock, including a correlation-based scheme, a flat-surface imaging scheme, and an image focus-based scheme.

The correlation-based scheme will be described first. Since the OCT A-mode scans/samples are collected while the SFE probe sweeps the object at the edge, $z(t_0)$, the adjacent A-mode lines $z(t_{\pm n})$, as shown in FIG. **8**, have a correlation relationship with the A-mode sample at $z(t_0)$. In the conceptual diagram **800** on the left of FIG. **8**, the trigger $z(t_0)$ sample is synchronized, aligned in the middle, while in diagram **810** on the right the samples are offset by two samples. As illustrated, 10 additional samples $z(t_{\pm n})$, where n=1 to 5) are collected around the trigger $z(t_0)$ with the same time interval.

The Line-to-Line correlation (L-L correlation) would be between one OCT scan/sample and its nearest neighbors, which would minimize when the A-line triggers are at perfect alignment of the phase angle of the B-mode scan. The Neighbor-to-Neighbor correlation (N-N correlation) would be maximum at the same point, as the two nearest neighbors would be looking at the same target region (assuming no probe motion). A graph **900** of the N-N correlation **910** and L-L correlation **920** is illustrated in FIG. **9**. By continuously generating L-L correlation and N-N correlation waveforms and adjusting the phase angle correction factor (slowly and filtered) to minimize L-L correlation and maximize N-N correlation, the OCT system may be stabilized for drift, such as by adjusting the offset **710**.

The flat-surface imaging scheme will next be described. When a flat surface is imaged using the OCT B-mode scan of the OCT system, the surface on the image should be a flat or straight line **1000**, as shown on the left side of FIG. **10**, provided the B-mode scan is synchronized with the spectrometer trigger at the edge of the B-mode scan. However, if the trigger is off from the edge of the B-mode scan (i.e., either earlier or later), resulting in a negative or positive phase delay, the image span may be reduced by the miss-alignment of the trigger. The resulting image, the non-straight line **0101** on the right side of FIG. **10**, will illustrate the amount of phase delay. By adjusting the phase offset **710** from the calibrated value until the flat surface image is a straight line, the synchronized trigger point can be obtained.

The image focus-based scheme will now be described. When the ideal phase angle for sampling is in place, the lateral extent of any feature at a give depth is at a minimum. This is because the fiber angle change (from one end of a line sample to the other end of the line sample) is maximized. If the spectrometer trigger is synchronized to the edge of the B-mode scan, the image has optimum focus, which may be illustrated from the image **1100** on the left of FIG. **11**. If the trigger is not synchronized to the edge, due the spectrometer exposure time, the spectrometer response is collected while the fiber is move, thereby causing the image to be less focused, as shown by image **1110** on the right side of FIG. **11**.

In an embodiment, lateral Fast Fourier Transforms (FFTs) of captured images at various phase angles around an optimum phase angle may be generated. An Artificial Intelligence (AI) system may then be utilized to analyze the FFTs of the images and identify the image with the optimum phase angle, which information may then be used to synchronize the trigger point, i.e. adjust the phase offset. An AI-based system **1200** may also be utilized to implement each one or all of the other schemes for synchronizing the trigger point as further illustrated in FIG. **12**.

As shown in FIG. **12**, A-mode lines (i.e., samples) may be collected and input to a B-mode image **1220** (which are created from the A-line scans) as well as an L-L correlation processor **1230** and an N-N correlation processor **1240**, operating in parallel. The output of the B-mode image **1220** may in turn be input to a lateral FFT processor **1250** and/or a straight-line processor **1260**, each also operating in parallel with the other processors. The output of each of the processors **1230**, **1240**, **1250** and **1260** may then be input to a previously trained AI engine that analyzes the input date and determines in real-time a phase correction for adjusting the spectrometer trigger.

FIG. **13** illustrates an embodiment for generating learning statistics for training the AI engine **1270** of FIG. **12**. As the SFE OCT scanning trigger clock is around 20 kHz, it is too high to be used in order to acquire A-line images for ground truth image sets. For AI training engine **1300** purposes, it may therefore be desirable to use a mechanical scanning probe system where the motor sweeping speed can be adjusted to acquire A-lines for either perfect (ground truth) image sets **1310** as well as aberrated (mis-aligned) image sets **1320**, i.e., images with acquisition phase errors. These image sets may then be fed into the AI training engine **1300**, along with decision parameters **1330** for each of the spectrometer trigger schemes, to generate learning statistics for training the AI engine **1270**.

FIG. **14** illustrates a relationship between motion induced reduction of lateral resolution and the radius of a B-mode scan (defined as the distance between the SFE probe and an imaging surface). The X-axis represents the B-mode scan radius (mm) on the imaging surface and Y-axis represents displacement of the probe during A-line acquisition time. Line **1440** represents the probe's moving distance during A-line acquisitions at each B-mode radius. For example, using a 5 microsecond acquisition window, at a 2.5 mm depth, the image would move 30 microns laterally. Horizontal lines **1410**, **1420**, **1430** represent lateral resolution based on a maximum B-mode scan radius. At a depth of 5 mm, represented by **1410**, the motion during acquisition would be 20 microns. Similarly, at a depth of 4 mm, **1420**, the motion during acquisition would be approximately 15 microns, and at a depth of 3 mm, **1430**, the motion would be approximately 12 microns. FIG. **15** illustrates absorption coefficients of tissue constituents, applicable to various embodiments and applications of the B-mode scans and methods discussed herein. The SFE probe transmits single mode laser lights for RGB and OCT imaging through the shared single mode fiber. The wavelengths of RGB are typically between 400-700 nm and OCT is between 900-1300 nm. The appropriate single mode fiber and OCT wavelength should be chosen to transmit both RGB and OCT in single mode without significant loss or mode changes (to multimode). FIG. **15** illustrates that in the 700-1100 nm wavelength range, the average absorption rate of materials is less than 10%, thus being particularly applicable for vascular applications.

FIG. **16** illustrates an exemplary computing environment in which embodiments of the present invention is depicted and generally referenced as computing environment **1600**. As utilized herein, the phrase "computing system" generally refers to a dedicated computing device with processing power and storage memory, which supports operating software that underlies the execution of software, applications, and computer programs thereon. As shown by FIG. **16**, computing environment **1600** includes bus **1610** that directly or indirectly couples the following components: memory **1620**, one or more processors **1630**, I/O interface **1640**, and network interface **1650**. Bus **1610** is configured to communicate, transmit, and transfer data, controls, and commands between the various components of computing environment **1600**.

Computing environment **1600**, such as a PC, typically includes a variety of computer-readable media. Computer-readable media can be any available media that is accessible by computing environment **1600** and includes both volatile and nonvolatile media, removable and non-removable media. Computer-readable media may comprise both computer storage media and communication media. Computer storage media does not comprise, and in fact explicitly excludes, signals per se.

Computer storage media includes volatile and nonvolatile, removable and non-removable, tangible and non-transient media, implemented in any method or technology for storage of information such as computer-readable instructions, data structures, program modules or other data. Computer storage media includes RAM; ROM; EE-PROM; flash memory or other memory technology; CD-ROMs; DVDs or other optical disk storage; magnetic cassettes, magnetic tape, magnetic disk storage or other magnetic storage devices; or other mediums or computer storage devices which can be used to store the desired information, and which can be accessed by computing environment **1600**.

Communication media typically embodies computer-readable instructions, data structures, program modules or other data in a modulated data signal such as a carrier wave or other transport mechanism and includes any information delivery media. The term "modulated data signal" means a signal that has one or more of its characteristics set or changed in such a manner as to encode information in the signal. By way of example, communication media includes wired media, such as a wired network or direct-wired connection, and wireless media, such as acoustic, RF, infrared and other wireless media. Combinations of any of the above should also be included within the scope of computer-readable media.

Memory **1620** includes computer-storage media in the form of volatile and/or nonvolatile memory. The memory may be removable, non-removable, or a combination thereof. Memory **1620** may be implemented using hardware devices such as solid-state memory, hard drives, optical-disc drives, and the like. Computing environment **1600** also includes one or more processors **1630** that read data from various entities such as memory **1620**, I/O interface **1640**, and network interface **1650**.

I/O interface **1640** enables computing environment **1600** to communicate with different input devices and output devices. Examples of input devices include a keyboard, a pointing device, a touchpad, a touchscreen, a scanner, a microphone, a joystick, and the like. Examples of output devices include a display device, an audio device (e.g. speakers), a printer, and the like. These and other I/O devices are often connected to processor **1610** through a serial port interface that is coupled to the system bus, but may be connected by other interfaces, such as a parallel port, game port, or universal serial bus (USB). A display device can also be connected to the system bus via an interface, such as a video adapter which can be part of, or connected to, a graphics processor unit. I/O interface **1640** is configured to coordinate I/O traffic between memory **1620**, the one or more processors **1630**, network interface **1650**, and any combination of input devices and/or output devices.

Network interface **1650** enables computing environment **1600** to exchange data with other computing devices via any suitable network. In a networked environment, program modules depicted relative to computing environment **1600**, or portions thereof, may be stored in a remote memory storage device accessible via network interface **1650**. It will be appreciated that the network connections shown are exemplary and other means of establishing a communications link between the computers may be used.

It is understood that the term circuitry used through the disclosure can include specialized hardware components. In the same or other embodiments circuitry can include microprocessors configured to perform function(s) by firmware or

switches. In the same or other example embodiments circuitry can include one or more general purpose processing units and/or multi-core processing units, etc., that can be configured when software instructions that embody logic operable to perform function(s) are loaded into memory, e.g., RAM and/or virtual memory. In example embodiments where circuitry includes a combination of hardware and software, an implementer may write source code embodying logic and the source code can be compiled into machine readable code that can be processed by the general purpose processing unit(s). Additionally, computer executable instructions embodying aspects of the invention may be stored in ROM EEPROM, hard disk (not shown), RAM, removable magnetic disk, optical disk, and/or a cache of processing unit. A number of program modules may be stored on the hard disk, magnetic disk, optical disk, ROM, EEPROM or RAM, including an operating system, one or more application programs, other program modules and program data. It will be appreciated that the various features and processes described above may be used independently of one another or may be combined in various ways. All possible combinations and sub-combinations are intended to fall within the scope of this disclosure.

Conditional language used herein, such as, among others, "can," "could," "might," "may," "e.g.," and the like, unless specifically stated otherwise, or otherwise understood within the context as used, is generally intended to convey that certain embodiments include, while other embodiments do not include, certain features, elements, and/or steps. Thus, such conditional language is not generally intended to imply that features, elements and/or steps are in any way required for one or more embodiments or that one or more embodiments necessarily include logic for deciding, with or without author input or prompting, whether these features, elements and/or steps are included or are to be performed in any particular embodiment. The terms "comprising," "including," "having," and the like are synonymous and are used inclusively, in an open-ended fashion, and do not exclude additional elements, features, acts, operations, and so forth. Also, the term "or" is used in its inclusive sense (and not in its exclusive sense) so that when used, for example, to connect a list of elements, the term "or" means one, some, or all of the elements in the list.

In an embodiment, a method for synchronizing an Optical Coherence Tomography (OCT) system, comprising detecting when a plurality of A-line scans obtained from reflected light of a cantilever scanning fiber within a probe oscillating along a scanning path that increases in amplitude over time are no longer being obtained at a point along the oscillating scanning path when the scanning fiber reaches a minimum speed; determining a value by which a phase angle of the oscillating scanning path is out of synchronization with the plurality of A-line scans; and adjusting a trigger clock for the obtaining the plurality of A-line scans based on the value.

In the embodiment, wherein the detecting includes obtaining a series of samples of at least one A-line scan among the plurality of A-lines scans just before, during and after the scanning fiber reaches the minimum speed, generating a Line-to-Line (L-L) correlation between at least one sample among the series of samples and nearest neighbor samples to the at least one sample among the series of samples, and generating a Neighbor-to-Neighbor (N-N) correlation between the at least one sample and two nearest neighbor samples, and wherein determining includes adjusting the value to minimize the L-L correlation and to maximize the N-N correlation.

In the embodiment, wherein the detecting includes inputting the plurality of A-line scans to an L-L processor and to an N-N processor operating in parallel with the L-L processor in order to generate the L-L correlation and the N-N correlation, and wherein the determining includes outputting the L-L correlation and the N-N correlation to a trained Artificial Intelligence (AI) engine to adjust the value in real-time.

In the embodiment, wherein the plurality of A-line scans are obtained from reflected light from a flat surface, wherein detecting includes determining if a B-line scan image constructed from the plurality of A-line scans is a straight line or a non-straight line, and wherein when the image is a non-straight line the determining includes further or alternatively adjusting the value until the non-straight line becomes the straight line.

In the embodiment, wherein the detecting includes inputting the plurality of A-line scans to an L-L processor and to an N-N processor operating in parallel with the L-L processor in order to generate the L-L correlation and the N-N correlation, constructing B-line scan images from a series of the plurality of A-line scans, and outputting the B-line scan images to a processor operating in parallel with the L-L processor and the N-N processor for analyzing whether each image among the B-line scan images is the straight line or the non-straight line, and wherein the determining includes outputting the L-L correlation, the N-N correlation, and a straight/non-straight line determination to a trained Artificial Intelligence (AI) engine to determine how to adjust the value in real-time.

In the embodiment, wherein the plurality of A-line scans are obtained from reflected light from a flat surface, wherein detecting includes determining if a B-line scan image constructed from the plurality of A-line scans is a straight line or a non-straight line, and wherein when the image is a non-straight line the determining includes adjusting the value until the non-straight line becomes the straight line.

In the embodiment, wherein the detecting includes constructing B-line scan images from a series of the plurality of A-line scans and outputting the B-line scan images to a processor for analyzing whether each image among the B-line scan images is the straight line or the non-straight line, and wherein the determining includes outputting a straight/non-straight line determination to a trained Artificial Intelligence (AI) engine to adjust the value in real-time.

In the embodiment, wherein the plurality of A-line scans are obtained from reflected light from a surface that is not a flat surface, wherein detecting includes determining if B-line scan images constructed from the plurality of A-line scans are in focus or out of focus, and wherein when the B-line scan images are out of focus the determining includes adjusting the value until one of the B-line scan images becomes in focus.

In the embodiment, wherein the determining includes generating Fast Fourier Transforms (FFTs) of a series of B-line scan images when the plurality of A-line scans are at various phase angles around an optimum phase angle, and analyzing the FFTs to determine if the B-line scan images are in focus or out of focus, and wherein the determining includes outputting an in focus/out of focus determination to a trained Artificial Intelligence (AI) engine to adjust the value in real-time.

In the embodiment, wherein the detecting includes obtaining a series of samples of at least one A-line scan among the plurality of A-lines scans just before, during and after the scanning fiber reaches the minimum speed, generating a Line-to-Line (L-L) correlation between at least one sample

among the series of samples and nearest neighbor samples to the at least one sample among the series of samples, and generating a Neighbor-to-Neighbor (N-N) correlation between the at least one sample and two nearest neighbor samples, and wherein the determining includes further or alternatively adjusting the value to minimize the L-L correlation and to maximize the N-N correlation.

In the embodiment, wherein the plurality of A-line scans are obtained from reflected light from a flat surface, wherein detecting includes determining if a B-line scan image constructed from the plurality of A-line scans is a straight line or a non-straight line, and wherein when the image is a non-straight line the determining includes further or alternatively adjusting the value until the non-straight line becomes the straight line.

In the embodiment, wherein the detecting includes generating Fast Fourier Transforms (FFTs) of a series of B-line scan images when the plurality of A-line scans are at various phase angles around an optimum phase angle, analyzing with a lateral FFT processor the FFTs to determine if the B-line scan images are in focus or out of focus, inputting the plurality of A-line scans to an L-L processor and to an N-N processor operating in parallel with the L-L processor in order to generate the L-L correlation and the N-N correlation, constructing B-line scan images from a series of the plurality of A-line scans; and outputting the B-line scan images to a processor operating in parallel with the L-L processor, the N-N processor and the lateral FFT processor for analyzing whether each image among the B-line scan images is the straight line or the non-straight line, and wherein the determining includes outputting the L-L correlation, the N-N correlation, a straight/non-straight line determination and an in focus/out of focus determination to a trained Artificial Intelligence (AI) engine to determine how to adjust the value in real-time.

In the embodiment, wherein the plurality of A-line scans are obtained from reflected light from a flat surface, wherein detecting includes determining if a B-line scan image constructed from the plurality of A-line scans is a straight line or a non-straight line, and wherein when the image is a non-straight line the determining includes further or alternatively adjusting the value until the non-straight line becomes the straight line.

In the embodiment, wherein the detecting includes generating Fast Fourier Transforms (FFTs) of a series of B-line scan images when the plurality of A-line scans are at various phase angles around an optimum phase angle, analyzing with a lateral FFT processor the FFTs to determine if the B-line scan images are in focus or out of focus, and outputting the B-line scan images to a processor operating in parallel with the lateral FFT processor for analyzing whether each image among the B-line scan images is the straight line or the non-straight line, and wherein the determining includes outputting an in focus/out of focus determination and a straight/non-straight line determination to a trained Artificial Intelligence (AI) engine to determine how to adjust the value in real-time.

While certain example embodiments have been described, these embodiments have been presented by way of example only and are not intended to limit the scope of the inventions disclosed herein. Thus, nothing in the foregoing description is intended to imply that any particular feature, characteristic, step, module, or block is necessary or indispensable. Indeed, the novel methods and systems described herein may be embodied in a variety of other forms; furthermore, various omissions, substitutions and changes in the form of the methods and systems described herein may be made without departing from the spirit of the inventions disclosed herein. The accompanying claims and their equivalents are intended to cover such forms or modifications as would fall within the scope and spirit of certain of the inventions disclosed herein.

What is claimed:

1. A method for synchronizing an Optical Coherence Tomography (OCT) system, comprising:

detecting when a plurality of A-line scans obtained from reflected light of a cantilever scanning fiber within a probe oscillating along a scanning path that increases in amplitude over time are no longer being obtained at a point along the oscillating scanning path when the scanning fiber reaches a minimum speed;

determining a value by which a phase angle of the oscillating scanning path is out of synchronization with the plurality of A-line scans; and

adjusting a trigger clock for the obtaining the plurality of A-line scans based on the value.

2. The method of claim **1**, wherein the detecting includes:

obtaining a series of samples of at least one A-line scan among the plurality of A-lines scans just before, during and after the scanning fiber reaches the minimum speed;

generating a Line-to-Line (L-L) correlation between at least one sample among the series of samples and nearest neighbor samples to the at least one sample among the series of samples; and

generating a Neighbor-to-Neighbor (N-N) correlation between the at least one sample and two nearest neighbor samples; and

wherein determining includes adjusting the value to minimize the L-L correlation and to maximize the N-N correlation.

3. The method of claim **2**, wherein the detecting includes:

inputting the plurality of A-line scans to an L-L processor and to an N-N processor operating in parallel with the L-L processor in order to generate the L-L correlation and the N-N correlation; and

wherein the determining includes outputting the L-L correlation and the N-N correlation to a trained Artificial Intelligence (AI) engine to adjust the value in real-time.

4. The method of claim **2**, wherein the plurality of A-line scans are obtained from reflected light from a flat surface, wherein detecting includes determining if a B-line scan image constructed from the plurality of A-line scans is a straight line or a non-straight line, and wherein when the image is a non-straight line the determining includes further or alternatively adjusting the value until the non-straight line becomes the straight line.

5. The method of claim **4**, wherein the detecting includes:

inputting the plurality of A-line scans to an L-L processor and to an N-N processor operating in parallel with the L-L processor in order to generate the L-L correlation and the N-N correlation;

constructing B-line scan images from a series of the plurality of A-line scans; and

outputting the B-line scan images to a processor operating in parallel with the L-L processor and the N-N processor for analyzing whether each image among the B-line scan images is the straight line or the non-straight line; and

wherein the determining includes outputting the L-L correlation, the N-N correlation, and a straight/non-

straight line determination to a trained Artificial Intelligence (AI) engine to determine how to adjust the value in real-time.

6. The method of claim **1**, wherein the plurality of A-line scans are obtained from reflected light from a flat surface, wherein detecting includes determining if a B-line scan image constructed from the plurality of A-line scans is a straight line or a non-straight line, and wherein when the image is a non-straight line the determining includes adjusting the value until the non-straight line becomes the straight line.

7. The method of claim **6**, wherein the detecting includes:

constructing B-line scan images from a series of the plurality of A-line scans; and

outputting the B-line scan images to a processor for analyzing whether each image among the B-line scan images is the straight line or the non-straight line; and

wherein the determining includes outputting a straight/non-straight line determination to a trained Artificial Intelligence (AI) engine to adjust the value in real-time.

8. The method of claim **1**, wherein the plurality of A-line scans are obtained from reflected light from a surface that is not a flat surface, wherein detecting includes determining if B-line scan images constructed from the plurality of A-line scans are in focus or out of focus, and wherein when the B-line scan images are out of focus the determining includes adjusting the value until one of the B-line scan images becomes in focus.

9. The method of claim **8**, wherein the determining includes:

generating Fast Fourier Transforms (FFTs) of a series of B-line scan images when the plurality of A-line scans are at various phase angles around an optimum phase angle; and

analyzing the FFTs to determine if the B-line scan images are in focus or out of focus; and

wherein the determining includes outputting an in focus/out of focus determination to a trained Artificial Intelligence (AI) engine to adjust the value in real-time.

10. The method of claim **8**, wherein the detecting includes:

obtaining a series of samples of at least one A-line scan among the plurality of A-lines scans just before, during and after the scanning fiber reaches the minimum speed;

generating a Line-to-Line (L-L) correlation between at least one sample among the series of samples and nearest neighbor samples to the at least one sample among the series of samples; and

generating a Neighbor-to-Neighbor (N-N) correlation between the at least one sample and two nearest neighbor samples;

and wherein the determining includes further or alternatively adjusting the value to minimize the L-L correlation and to maximize the N-N correlation.

11. The method of claim **10**, wherein the plurality of A-line scans are obtained from reflected light from a flat surface, wherein detecting includes determining if a B-line scan image constructed from the plurality of A-line scans is a straight line or a non-straight line, and wherein when the image is a non-straight line the determining includes further or alternatively adjusting the value until the non-straight line becomes the straight line.

12. The method of claim **11**, wherein the detecting includes:

generating Fast Fourier Transforms (FFTs) of a series of B-line scan images when the plurality of A-line scans are at various phase angles around an optimum phase angle;

analyzing with a lateral FFT processor the FFTs to determine if the B-line scan images are in focus or out of focus;

inputting the plurality of A-line scans to an L-L processor and to an N-N processor operating in parallel with the L-L processor in order to generate the L-L correlation and the N-N correlation;

constructing B-line scan images from a series of the plurality of A-line scans; and

outputting the B-line scan images to a processor operating in parallel with the L-L processor, the N-N processor and the lateral FFT processor for analyzing whether each image among the B-line scan images is the straight line or the non-straight line; and

wherein the determining includes outputting the L-L correlation, the N-N correlation, a straight/non-straight line determination and an in focus/out of focus determination to a trained Artificial Intelligence (AI) engine to determine how to adjust the value in real-time.

13. The method of claim **8**, wherein the plurality of A-line scans are obtained from reflected light from a flat surface, wherein detecting includes determining if a B-line scan image constructed from the plurality of A-line scans is a straight line or a non-straight line, and wherein when the image is a non-straight line the determining includes further or alternatively adjusting the value until the non-straight line becomes the straight line.

14. The method of claim **11**, wherein the detecting includes:

generating Fast Fourier Transforms (FFTs) of a series of B-line scan images when the plurality of A-line scans are at various phase angles around an optimum phase angle;

analyzing with a lateral FFT processor the FFTs to determine if the B-line scan images are in focus or out of focus; and

outputting the B-line scan images to a processor operating in parallel with the lateral FFT processor for analyzing whether each image among the B-line scan images is the straight line or the non-straight line; and

wherein the determining includes outputting an in focus/out of focus determination and a straight/non-straight line determination to a trained Artificial Intelligence (AI) engine to determine how to adjust the value in real-time.

* * * * *